

Total Skin Electron Therapy: A Modified Technique for Small Room Linear Accelerator

TAREK SHOUMAN, M.D. and ZEINAB EL-TAHER, Ph.D.

The Department of Radiation Oncology, National Cancer Institute, Cairo University

ABSTRACT

Objective: Development of a technique for treating whole-body skin using linear accelerator with electron beam energy of 6-MeV at a short treatment distance.

Material and Methods: The 6 MeV high dose rate total skin electron irradiation mode on a linear accelerator was used. Beam profiles and percentage depth doses in the patient plane were measured for different beam angulations.

Results: At a treatment distance (SSD) of 292cm and using acrylic scatterer-degrader 4mm thick, the beam penetration was calculated so that the 80% dose lied at 1.6cm for the single beam and only 6mm for the clinical beam. A uniform vertical profile was obtained by using 3 beams for each treatment position with gantry angles of 700, 900 and 1100.

Conclusions: We could implement a modified stanford technique for total skin electron beam irradiation at a short treatment distance. Using an acrylic scatterer-degrader and three beam angulations we could produce a uniform beam in the treatment plane.

Key Words: Total skin irradiation - Mycosis Fungoides - Electron beam.

INTRODUCTION

Total body skin irradiation with low energy electrons has been used for the treatment of mycosis fungoides since the 1950s [1]. Several different techniques have been developed at various centers and these are described in a report published by the American Association of Physicists in Medicine (AAPM) [2].

The main objective of the treatment is to treat uniformly the entire surface of the body to a limited depth. To achieve this, the electron field at the treatment plane should cover an area 200cm at least in height and 80cm at least in width to encompass large patients. Since varia-

tion in the shape, orientation, and size of the body makes it difficult to obtain adequate dose uniformity over the entire body surface, two to six overlapping fields [3-5] are often employed. The original Stanford technique pioneered by Karzmark et al. [6] employed four body orientations, anterior, posterior, and lateral fields of a standing patient. This technique was later modified by Page et al. [5] to obtain a better dose uniformity and the original set-up was replaced by a six-field technique.

In the present work, we describe the development of a total skin electron beam technique (TSEB) and the choice of beam angulations and scatterer that produce adequate beam uniformity and penetration according to the short treatment distance of our linear accelerator room.

MATERIAL AND METHODS

At the National Cancer Institute (NCI), Radiation Oncology Department, the TSEB program was set-up using 6 MeV electron beam from Varian clinac 1800 linear accelerator. The TSEB technique chosen was similar to the modified Standford technique [5] but with variation of the gantry angles used along the irradiation fields. The patient was standing at a distance of 292cm from the rotation axis of the accelerator on a rotating platform that was designed to rotate 60° apart to facilitate the six patient positions orientation.

The patients were irradiated from six different directions. On the first day of treatment, anterior and two posterior oblique fields were applied while on the following day posterior and two anterior oblique fields were applied to

cover the whole length of the patient. Three fields were used along each of the six positions, one portal with 90° gantry angle directed to the patient, a superior and an inferior portals directed 20° above and below the horizontal axis using angles 70° and 110°, respectively. Figs (1,2) demonstrate the patient positions during TSEB.

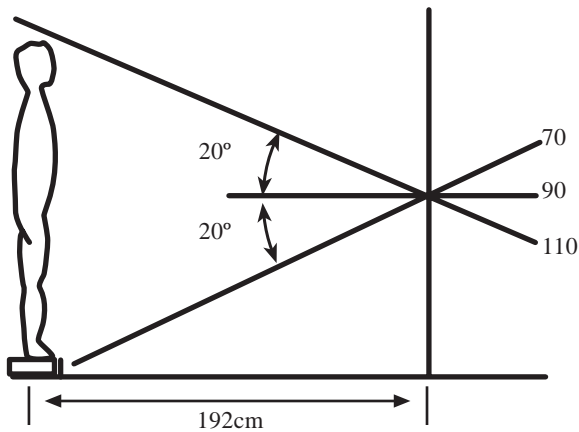


Fig. (1): Patient standing at a distance of 192cm from the isocenter of the accelerator.

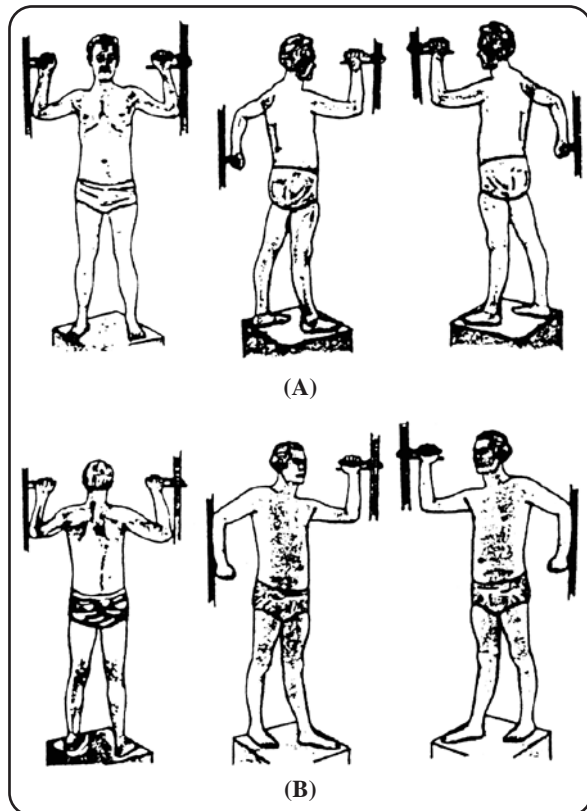


Fig. (2) A: Positions of the patient in first day.
 B: Positions of the patient in second day.
 Niroomand et al. [16].

The eyes, nails and toes were protected during irradiation using a 2mm thick lead shields that were designed in the mould room. Only in patients with eye lids skin affection, internal gold eye shields covered with wax were used instead of the external eye shields. On the other hand, the areas that received an additional booster dose were mainly soles of feet, perineal region, inframmary area in female patient and vertex of scalp. The dose delivered to these areas were measured using thermoluminescent dosimeters (TLD) during the treatment session of TSEB.

Electron Beam Uniformity:

The electron beam was diffused with the use of a scatterer in order to get an acceptable flat field. Without this scatterer, the beam intensity would be forwardly peaked. With normal sized fields (e.g. 21 x 21cm) no lack of uniformity was detected across the field. However, when we used an extended SSD and 1 x 2sq.m. field, the central axis part of the beam showed a higher intensity than the periphery. This observation was detected when applying X-omat films on the wall behind the patient position and irradiating them serially. These films were developed and the beam flatness was then read by the use of the denistometer.

Degradation of the beam energy was also achieved with the use of a scatterer, so that calculation was made to determine the required scatterer thickness that would provide adequate beam spoiling (reduction of average beam energy) and scattering. The scattering material was made of presspex since it is transparent and facilitates patient monitoring. It is of low Z material i.e. no bremsstrahlung X-ray production. It is flexible, strong and durable. It has a known stopping power that can be tabulated so that beam degradation through the presspex could be easily calculated. The dimensions of the sheet used were 260 x 150cm. The scatterer was suspended from three hooks attached to the ceiling just in front of the patient.

For dose rate evaluation, a Mrakus chamber model PTW (# N23343) was used along with an unidose PTW electrometer [7]. The chamber was put at the patient treatment distance at the level of LINAC isocenter height. Film dosimetry was performed with X-omat verification film by Kodak and using a Kodak developer.

X-ray Contamination:

The X-ray contamination was measured. A depth dose curve was plotted at the patient position with the gantry fixed at 90 degrees, the tail of the percentage depth dose (PDD) consisted mainly of cable induced charges and to lesser extent bremsstrahlung contamination. To separate the bremsstrahlung from the cable effect, the markus electron chamber was placed at the patient position and shielded with 10cm of plastic and 10cm of lead. On turning the beam on, the reading on the electrometer would be the pure cable signal since with that set-up no radiation could enter the chamber's sensitive volume. This chamber signal was recorded and subtracted from all subsequent depth dose readings yielding electron plus X-ray dose.

Dose Measurements:

In vivo, dosimetric measurement of TSEBT was important for the determination of the distribution of the dose to the patient's skin and verifying that the prescribed dose was correct. Film dosimetry was chosen. A RANDO-thropomorphic phantom was used and a film was cut and introduced into RANDO along a transverse plane at the navel height. Then RANDO was placed at the patient position (292cm SSD). The 18 fields were applied and 200 MU was delivered per field. Six fields were delivered with a gantry angle of 110°, six fields at 90° and the last six fields were at 70°. The film was then retrieved from RANDO and developed. The radiation pattern on the film was that of a black ring similar to that shown in Fig. (3). The films were scanned using Wellpofer Densitometer (WP102) to determine the PDD and isodose curves.

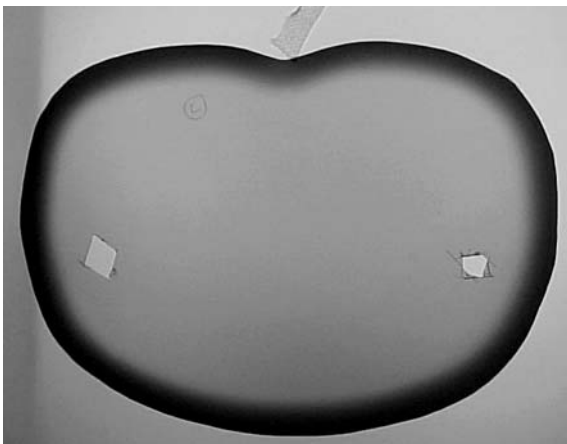


Fig. (3): Film dosimetry in a rando phantom, illustrating the homogenous distribution of the irradiation.

According to the American Association of Physicists in Median Task Group AAPM report No. 23 recommendations [2], we adopted the following steps to determine the patient dose. At first we selected several different radii on the film and evaluated the maximum optical density (OD) along each radius. All OD maximum values were averaged and the average OD was used to represent the patient dose. Then we converted the OD to a dose by the use of an H and D curve (Hurter and Driffield) which is sensitometric curve (optical density as a function of absorbed dose) (Fig. 4). To construct an H and D curve, we irradiated a series of films to certain doses of certain energy. The resulting optical densities were then read and OD was plotted versus absorbed dose.

To achieve this, the films were placed at the patient position where the dose rate for a single field with 90° gantry angle, was known to be 0.05695 cGy/Mu. This dose rate was obtained using a parallel plate chamber with a polystyrene phantom. A depth dose curve was drawn by taking readings at different depths. At each depth, two readings were taken, one with a positive bias (+300 volts) to the chamber and the other with a negative bias (-300 volts). Both readings were corrected for extracamer current contributed by the cable. The two readings were then averaged in order to correct for the polarity effect which was appreciable in this experiment. Once this was done, a depth dose curve (Fig. 5) was plotted and the mean energy E_0 was calculated from the R_{50} (the depth at which the dose is 50% of the max. dose):

$$R_{50} = 1.25\text{cm}$$

$$E_0 = C \times R_{50}$$

$$E_0 = 2.33 \text{ MeVcm}^{-1} \times 1.25\text{cm} = 2.91 \text{ MeV}$$

The absorbed dose at 4mm depth (d_{max}) was calculated and corrected according to AAPM task group (21) as follows:

$$D_{\text{poly/U}} = M/U \times C_{t,p} \times N_{\text{gas}} \times (L/P)^{\text{poly}}_{\text{air}} \times \text{Prepl} \times P_{\text{ion}} \times P_{\text{wall}}$$

$$D_{\text{water/U}} = D_{\text{poly/U}} \times (S/P)^{\text{poly}}_{\text{air}} \times \Phi^{\text{poly}}_{\text{air}}$$

The absorbed dose at 4mm depth (d_{max}) = 0.05695 cGy/Mu.

After calculating the dose at the patient position we were able to irradiate the films and draw an H and D curve. The data points for the H & D curve were located at 10, 30, 45, 60, 80 and 110 cGy as shown in (Fig. 4). Eighteen fields of radiation (200 MU each) were delivered to RANDO. The average OD was found to be 1.47, which was equivalent to 55 cGy. Then by dividing 55 cGy/3600 MU = 0.0153 cGy/MU total. Since the prescribed dose was 175 cGy/fraction so that the calculated total MU required was 175 cGy/0.0153 cGy/MU = 11438 MU. Then to get MU per each field, we divided 11438 MU/18 fields = 635 Mu per field.

According to the final measurements for the PDD of TSEBT at 292cm, it was found that, the maximum depth was 4.5mm and the practical range Rpequaled 1.8cm. The most probable energy was calculated as follows:

$$E_p = a_0 + a_1 RP + a_2 (RP)^2$$

a_0, a_1 and a_2 are constants.

$$= 0.22 + 1.98 \times 1.8 + 0.0025 \times (1.8)^2 = 3.79 \text{ MeV.}$$

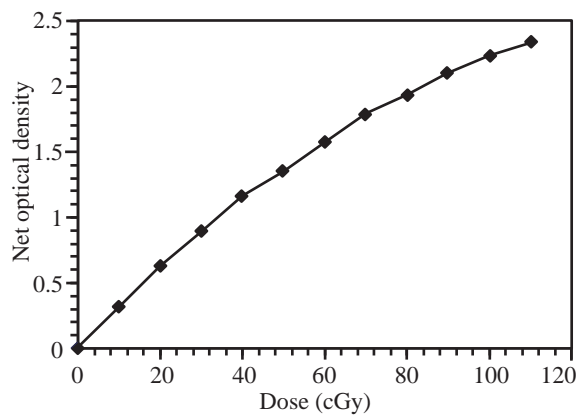


Fig. (4): H and D curve (optical density as a function of absorbed dose).

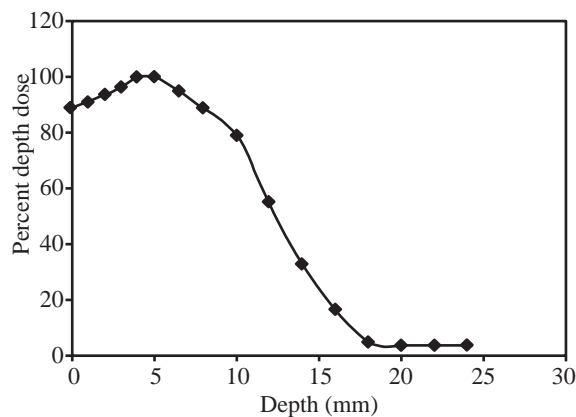


Fig. (5): Percentage depth dose for TSEB at SSD 292cm from a single beam.

RESULTS

The body section of the RANDO-Alderson phantom was used to measure the depth dose distribution of TSEB using two, four and six fields techniques. All measurements were made at an SSD of 292cm similar to the clinical set-up. The used energy was 6 MeV and it was degraded to 3.8 MeV by placing perspex degrader 4mm thick and 20cm in front of the phantom. Both the surface and depth doses were measured using thermoluminescent dosimeters (TLDs) and film dosimetry. The results of film dosimetry and TLDs readings for a given set-up are presented in Fig. (6-A,B,C).

Point A in all the figures represented the axis of the incident beam and point B was the midpoint between two A points. Fig. (6-A) shows the dose distribution of the two-fields technique (anteroposterior and posteroanterior). With a beam of 3.8 MeV and an incidence angle of 90°, the entrance dose at point A was 86% of the maximum dose which was at a depth of 0.4cm. The incidence angle decreased towards the periphery of a curved surface and the 'D' max. shifted to shallower depths and ultimately reached the surface. At point B the superficial dose fell off rapidly to 35% compared to 86% of the entrance dose. This resulted from the increased distance that electrons must traverse in the phantom in order to reach positions along the radius and from the increased loss of electrons that were scattered out of the phantom for a near tangential incidence. In clinical practice this low dose at point B using two fields TSEB would result in high incidence of recurrences along the flanks.

Fig. (6-B) shows the dose distribution of four equally weighted fields TSEB (AP [Anterior-Posterior], PA [Posterior-Anterior] and 2 lateral fields). At point A the difference between the surface dose and 'D' max. markedly diminished because of the tangential electron contribution from the two lateral fields separated by 90° on each side. The surface dose at point A in the four-fields technique was 94% compared to 86% in the two-fields technique. The surface dose at point B in the four-fields technique was 130% with 'D' max. of 140% at 0.2cm. This was due to the contribution of the two adjacent fields. However, the depth dose at point B was slightly less than the depth dose at point A

because no electrons at point B entered at 90° and all the electrons entered tangentially at point B. In clinical practice this high dose at point B in four equally weighed fields TSEB may result in linear skin reactions, especially along the lower extremities.

Fig. (6-C) shows the dose distribution of the six-fields technique (AP [Anterior-Posterior], LPO [Left-Posterior-Oblique], RPO [Right-Posterior-Oblique], PA [Posterior-Anterior], LAO [Left-Anterior-Oblique], and RAO [Right-Anterior-Oblique]). At point A the 'D' max. started at the surface because of the increased tangential electron contribution from the adjacent fields separated by 60° on either side. The surface and superficial depth dose at point B was slightly lower than at point A because of the distance and all the electrons entered point B at an angle. However, the depth dose curves at both points were coincident at depths greater than 1cm. According to these results, we chose the six fields arrangement in our technique as it showed the best dosimetry.

In spite of the use of a scatterer to improve field flatness yet the measurements of the dose distribution using the dual portals, showed unhomogenous dose at the 10cm gap between the two portals with mixed areas of hot and cold spots. As a result, an additional method was implemented to improve dose distribution when three portals were used to irradiate along each one of the six directions mentioned previously. A field at 70 degree, a second field at 90 degree and a third at 110 degree with field size 21 x 21cm resulted in a flat curve. When we irradiated from six different directions, the original single field depth dose curve became drastically shallower. This was because many electrons entered the patient skin obliquely rather than perpendicularly. As a result the surface dose could increase drastically. We should note that the electron beam range did not change because it was determined by the energy of electrons that were impinging perpendicularly on the skin.

The single electron beam would show different degradation during its passage before entering the patient. The starting beam energy was 6 MeV. Then after passing 2 meters of air, this would subtract approximately 0.5 MeV from the beam leaving about 5.5 MeV. After

passing through the degrader (4mm), only 5 MeV would be left. Since approximately 80% depth dose was reduced by a factor of 66%, so 80% depth dose from a single field of 5 Mev would be at 1.6cm while from six fields would be at 6mm.

Thermoluminescent dosimetric measurements were done on the RANDO phantom in order to assure clinically acceptable dose uniformity at different anatomical sites. The readings showed variations of $\pm 10\%$ of the prescribed skin dose. TLD measurements was also done on 10 patients and showed a surface dose uniformity of $\pm 10\%$ of the prescribed dose. However, due to the variations in height and size of the patients together with the shielding effects of the legs upon each other and the arms upon the head, neck and trunk, it was recommended to evaluate the TLDs measurements for all patients throughout a full treatment cycle and identify the boost dose required to the underdosed areas individually. All locations which have flat surface on the body gave readings very close to 100% of the prescription dose. At the umbilicus (the prescription point), the average TLD measurement was 103% of the prescribed dose. There were variable readings obtained from several body surface sites including the perineum, under surface of the breasts and head top. In the perineum, most of the readings were only 20-30% of the prescription dose. The top of the head showed variations depending on the height of the patient whether tall or short with variation from 40%-60% of the prescription dose. The boost dose to the scalp vertex should be individually adjusted so as not to exceed 25 Gy to avoid permanent hair loss. For the areas under the breast in female patients, the variation in TLDs readings varied markedly according to the size of the breast. Women with large pendulous breasts had TLDs reading of about 40% of the prescribed dose and required a boost dose whereas women with smaller breast had an adequate dose to the tissues and required no boost.

Dosimetric measurements showed that the Bremsstrahlung contribution of the tail of the PDD curve was as low as 5%. In the beams overlap zones, the photon contamination was negligible. No special protection of the ovaries was therefore needed in female patients.

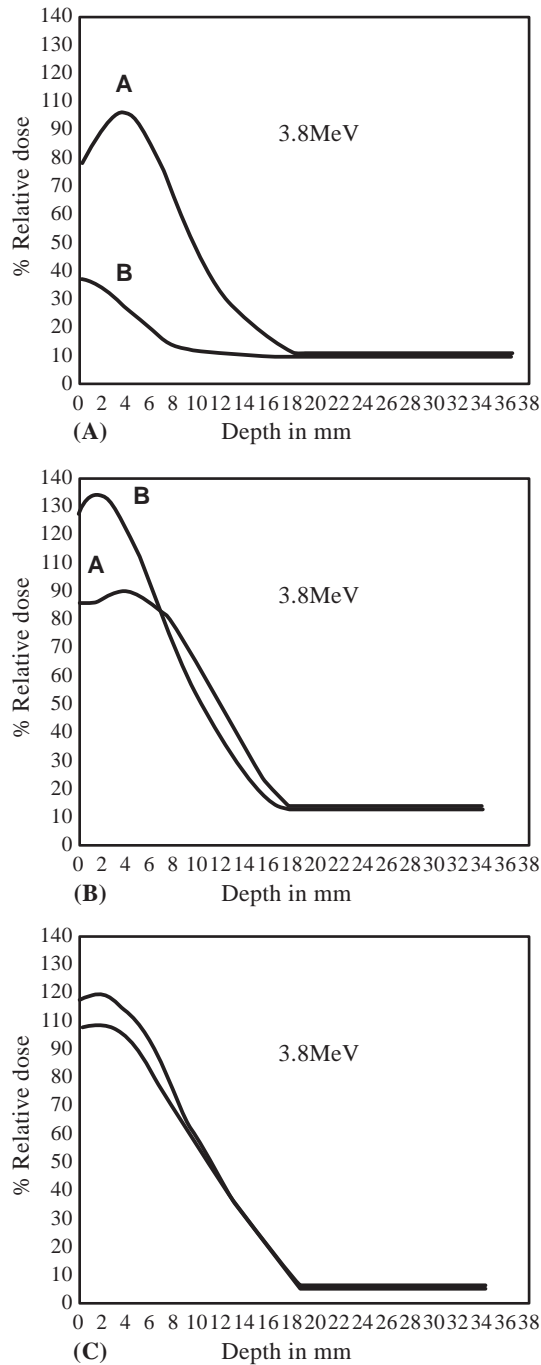


Fig. (6): The film dosimetry and the TLD readings for a given set-up: (A) Two-fields technique (B) Four-fields technique (C) Six-fields technique.

DISCUSSION

Once an institution decides to provide the TSEBT modality, an adequate technique must be chosen and commissioned. This depends on the availability of the equipment and on the

physical constraints imposed by the room design [8]. Most current treatments use low energy electron with a typical energy from 6 to 10 MeV at the wave guide window resulting in a sum of energy from 3.5 to 7 MeV at the position of the patient at the large nominal SSD (300-500cm) in the large TSEBT field [9].

At the NCI, Radiation Oncology Department, Varian 1800 linac is used. It gives an energy of 6 MeV at the wave guide resulting in an energy of 3.8 MeV at the patient position using nominal SSD of 292cm which suits the design of the treatment room. The modified Stanford technique used SSD of 410cm which was somewhat larger than the 305cm SSD used by the original Stanford [10]. The patients were treated in the standing position with the arms vertically stretched overhead, resulting in a flat field of approximately 2.5 meters in height. That was why the use of a single horizontally directed beam did not give sufficient dose uniformity at that vertical dimension.

To obtain a uniform beam intensity covering the patients from hands to feet, multiple electron fields were used with central rays of ± 20 degrees from the horizontal. An important point in the choice of multiple overlapping fields technique was the variation in the shape, orientation and size of the body of the patients that made it difficult to obtain adequate dose uniformity over the entire body surface. The Stanford technique used the six patient positions orientation with dual portals ± 20 degrees from the central ray (12 fields). At our institution, however we applied three portals for each field with the same degrees of beam angulation (18 fields). The reason for this modification was that the measurements of the dose distribution using the dual portals, showed unhomogenous dose at the 10cm gap between the two portals with mixed areas of hot and cold spots. On the other hand, the beam uniformity was achieved when applying the three portals with overlapping fields.

The depth dose distribution for the 12 fields of the Stanford technique showed that the 80% dose was at depth of 9mm for the single beam and only 3.5mm for the clinical beam [11]. That was slightly different from the technique applied in our center using 18 fields with the 80% dose situated at 1.6mm for the single beam and only 6mm for the clinical beam.

The dose homogeneity of the entire thickness of the infiltrated skin was an essential factor for effective treatment results. The cellular infiltration of the patch-plaque phase of MF tends mainly to localize primarily in the superficial portion of the skin (2-4mm), but it often extends into deeper regions around hair follicles and eccrine glands and may extend into subcutaneous tissues at a depth of 15mm or more with tumorous infiltration. This might result in an unhomogenous dose distribution within the whole skin thickness [12]. Differences in skin infiltration can be compensated for by varying the beam energies or by interposing appropriate thickness of tissue equivalent to the bolus. The first solution was better since the second solution involved less risk of dose variation induced by the oblique path of the beam in bolus. Even when using optimum technique low dose areas of varying degrees will still occur [13]. The beam energy used at our institution was inappropriate for treating tumorous lesions; so we recommended to set up a TSEB program at higher energies for the treatment of these patients.

In TSEB, the X-ray contamination resulting from the large electron fields was undesired with troublesome side effects that were overlooked or ignored. Experiments showed that the total Bremsstrahlung contamination to the dose at the midline of the patient undergoing TSEB was approximately twice the level measured for the single electron field used in TSEB. This dose doubling factor was found for both the multiple fields TSEB technique [14] and the rotational technique [15]. The X-ray contamination for a single TSEB beam, was about 4% of the prescribed electron dose or 1.6 Gy for a typical prescribed electron dose of 40 Gy [9]. At our institution, the resulting total X-ray contamination was about $\pm 5\%$ and which was quite acceptable.

With the Stanford technique it was possible to get lower X-ray background from the multiple angulated beam. The X-ray contamination was largest along the central ray axis and drops off rapidly as a function of distance away from the central ray axis. It was 0.2% of the maximum dose at midphantom position and was about 0.4% of the maximum dose at 70cm above and below the mid phantom positions [16].

In clinical practice, the actual variation of surface dose produced by the shape and orientation of the body surface with respect to the incident beams was greater than that of the phantom measurements. Surface cavities generally receive less dose than flat or convex surfaces. Thermoluminescent dosimetry and film dosimetry were both useful methods in the determination of the treatment skin dose rate as well as in the determination of the actual composite percentage depth doses for the clinical beams. TLD measurements was done on 10 patients and showed a surface dose uniformity of $\pm 10\%$ of the prescribed dose. However, due to the variations in height and size of the patients together with the shielding effects of the legs upon each other and the arms upon the head, neck and trunk, it was recommended to evaluate the TLDs measurements for all patients throughout the full treatment cycle and identify individually the boost dose required to the underdosed areas. For all women who undergo TSEB, TLDs should be placed under the breast to document the dose received and to determine the required boost field since the TLDs readings varied according to the size of the breast.

These variations in TLDs were similar to that reported by Weaver et al. [17]. They showed that among 22 patients treated with TSEB in the standing position using a six field technique to a dose of 35 to 40 Gy using degraded 9 MeV electron beam, the TLD, readings revealed dose variation amounting to $\pm 10\%$ of the prescribed dose. Thin areas of the body showed large deviations up to 22% of the prescription dose. Other special areas, such as the perineum and scalp vertex, showed variations up to 40% or more. Permanent loss of scalp hair was noticed in almost all patients receiving a scalp boost greater than 25 Gy.

Conclusion:

We successfully implemented a modified Stanford technique for TSEBT using LINAC- 6MeV with limited SSD according to treatment room dimensions. The dose uniformity was achieved by using scatterer-degrader mounted close to the patient and applying 3 angulated beams for each treatment position. The uniformity of patient dose was found to be comparable to that achieved by other TSEBT protocols described in the literature.

REFERENCES

- 1- Lo TCM, Salzman FA, Moschella SL, Tolman EL, Wright KA. Whole body surface electron irradiation in the treatment of mycosis fungoides. *Radiology*. 1979, 130: 453-457.
- 2- American Association of Physicists in Medicine Task Group 23. Total skin electron therapy: Technique and dosimetry. New York: American Institute of Physics. 1988, p: 25-33.
- 3- Edelstein GR, Clark T, Holt JG. Dosimetry for total body electron-beam therapy in the management of mycosis fungoides. *Radiology*. 1973, 108: 691-694.
- 4- Karzmark CJ. Physical aspects of whole-body superficial therapy with electrons. *Front Radiat Ther Oncol*. 1968, 2: 36-41.
- 5- Page V, Gardner A, Karzmark CJ. Patient dosimetry in the electron treatment of large superficial lesions. *Radiology*. 1970, 94: 635-641.
- 6- Karzmark CJ, Lovinger R, Steele RE. A technique for large-field, superficial electron therapy. *Radiology*. 1960, 74: 633-643.
- 7- Brahme A, Svensson H. specification of electron beam quality from the central-axis depth absorbed-dose distribution. *Med Phys*. 1976, 3: 95-102.
- 8- Ahix FH. Introduction to Radiological Physics and Dosimetry. New York, John Wiley & Sons. 1986, P: 213-225.
- 9- Podgorsak EB, Podgorsak MB. The Modern Technology of Radiation Oncology. Jacobe Van Dyk, Editor. The McGill rotational TSEI technique. 1999, p. 669-676.
- 10- Khan F. The physics of radiation Therapy, 2nd ed. Baltimore: Williams & Wilkins. 1994, P: 346-360.
- 11- Fraass BA, Roberson PL, Glatstein E. Whole-skin electron treatment: Patient skin dose distribution. *Radiol*. 1983, 146: 811-814.
- 12- Brady LW, Simpson LD, Day JL, Tapley N. Principles and Practice of Radiation Oncology. Third Edition edited by C.A. Perez and L.W. Brady. Lippincott-Raven Publishers, Philadelphia. 1997.
- 13- Meyn RE, Peters LJ, Mills MD. Radiological aspects of electron beams. In Vaeth JM, Meyer JL, eds. *Frontiers of Radiation Therapy and Oncology*. Vol 25. Basel: S Karger. 1991, 53-60.
- 14- Holt JG, Perry DJ. Some physical consideration in whole skin electron beam therapy. *Med Phys*. 1982, 9: 769-776.
- 15- Podgorsak EB, Pla C, Pla M, Lefebvre PY, Heese R. Physical aspects of a rotational total skin electron irradiation. *Med Phys*. 1983, 10:159-168.
- 16- Niroomannand A, Gillin MT, Komaki R, Kline RW, Grimm DF. Dose distribution in total skin electron beam irradiation using the six field technique. *Int J Rad Oncol Biol Phys*. 1986, 12: 415-419.
- 17- Weaver R, Gerbi B, Dusenbery K. Evaluation of dose variation during total skin electron irradiation using thermoluminescent dosimeters. *Int J Rad Oncol Biol Phys* 1995, 33:475-478.